ELSEVIER

Journal of Structural Geology 28 (2006) 99–114

JOURNAL OF STRUCTURAL GEOLOGY

www.elsevier.com/locate/jsg

Balancing and restoration of piercement structures: geologic insights from 3D kinematic models

Hongwei Yin [a,b,*], Richard H. Groshong Jr [b]

[a] *Department of Earth Sciences, Nanjing University, Nanjing, JiangSu 210093, People's Republic of China*
[b] *Department of Geological Sciences, University of Alabama, Tuscaloosa, AL 35487, USA*

Received 23 August 2004; received in revised form 1 September 2005; accepted 16 September 2005
Available online 2 November 2005

Abstract

Restoration of cross-sections and map surfaces of volume-balanced 3D flexural-slip models are presented to provide insight into the structural interpretation and validation of highly 3D structures like faulted salt domes. 2D restoration results in apparently unbalanced cross-sections. Most sections show apparent thickening on dome flanks because the section line is oblique to the dip, except the radial cross-section that bisects a flank horst or graben along the slip direction. A section is corrected by adjusting the thickness according to the true dip as determined in map view. A cross-section from the flank of a 3D piercement structure is best restored by flexural-slip unfolding between pin lines placed at each edge of the section. Parallel flexural-slip unfolding is a reasonably good and practical restoration method for 3D piercement structures. Small gaps nearly always exist along every fault trace restored in the model. This systemically distributed small inconsistency does not, however, indicate a problem in the interpretation. These small gaps are due to the use of the same unfolding direction for every restored block. Insights from model dome restoration are applied to test the interpretation of natural salt dome examples from eastern Texas and northern Germany.

Keywords: Salt dome; Kinematic model; Radial fault; Balancing and restoration

1. Introduction

Balancing and restoration have been widely used to test the viability and admissibility of geological interpretations and to predict alternative interpretations of deep or poorly imaged structures, which can be approached in 2D as section restoration and 2.5D as map-view restoration. The concepts of section balancing and restoration were first presented by Chamberlin (1910) and have been codified for thrust sheets and faulted folds (e.g. Dahlstrom, 1969; Woodward et al., 1989), extension structures (e.g. Gibbs, 1983; White et al., 1986), and, more recently, salt structures (e.g. Rowan and Kligfield, 1989; Brewer and Groshong, 1993; Hossack, 1995). One extension of the 2D techniques into three dimensions is the map-view restoration, which is called the 2.5D or pseudo 3D approach. Map-view restoration has been applied to structures with some out-of-section material movement (e.g. Barr, 1985; Gratier et al., 1991; Gratier and Gullier, 1993; Kerr et al., 1993; Rouby et al., 1993, 2000; Kerr and White, 1996; Buddin et al., 1997; Williams et al., 1997).

Both section and map-view restorations have been effective for structures that are fundamentally 2D. Will the same methods work with a truly 3D structure like a radially faulted circular dome that has different transport directions for each faulted block? To investigate the nature and magnitude of the potential problems in the balance and restoration of strongly 3D structures, we have balanced and restored a volume-balanced 3D flexural-slip model that we derived based on the properties of active piercement structures. The results provide insight not only into the restoration of salt domes, but also into the problems that may arise in the balance and restoration of any significantly 3D structure.

We begin the discussion with a brief review of salt piercement structures, followed by the description of our

* Corresponding author. Tel.: +86 25 8368 6759; fax: +86 25 8359 6016.
E-mail address: hwyin@nju.edu.cn (H. Yin).

0191-8141/$ - see front matter © 2005 Elsevier Ltd. All rights reserved.
doi:10.1016/j.jsg.2005.09.005

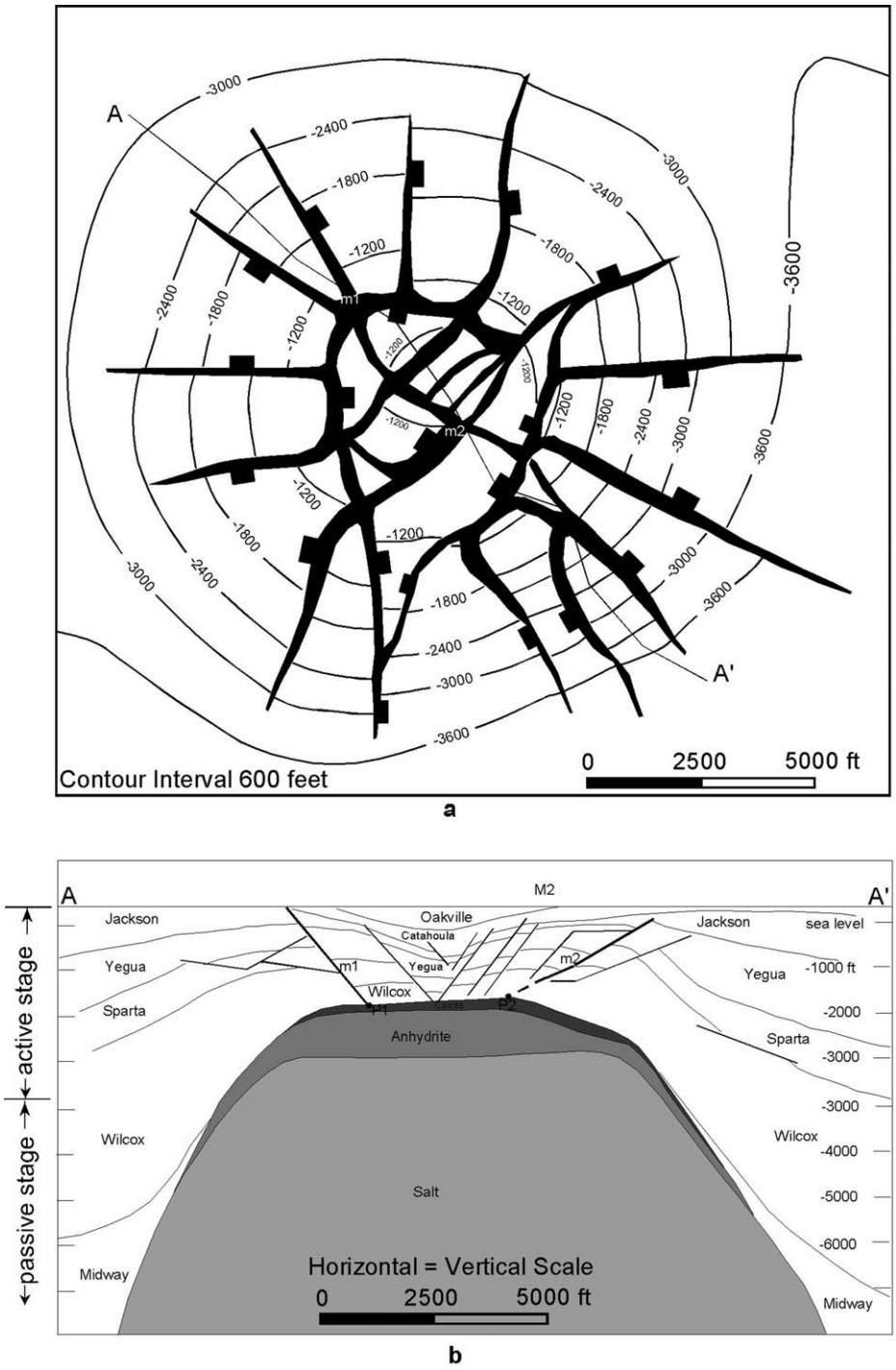

Fig. 1. Clay Creek dome (after McDowell, 1951). (a) Structure contour map drawn on top of the Wilcox Formation. (b) Structure section A–A′.

kinematic model of active salt domes. Model domes with two and three mutually offsetting normal faults have been constructed. To evaluate the admissibility of cross-section balancing and restoration technique when applied to domal structures, we show restored 2D sections cut from model domes in numerous orientations. Most sections from model domes appear to be unbalanced. A thickness adjustment method is suggested to fix the problem of apparent unbalance. In order to test the admissibility of map-view restoration techniques, a model dome with three major normal faults is restored using vertical simple shear and flexural-slip unfolding. Results show that for domal structures, flexural-slip unfolding is a reasonably good restoration method, while vertical simple shear is not. Insights from the analysis of model domes have been applied to test the viability of interpretations of two natural

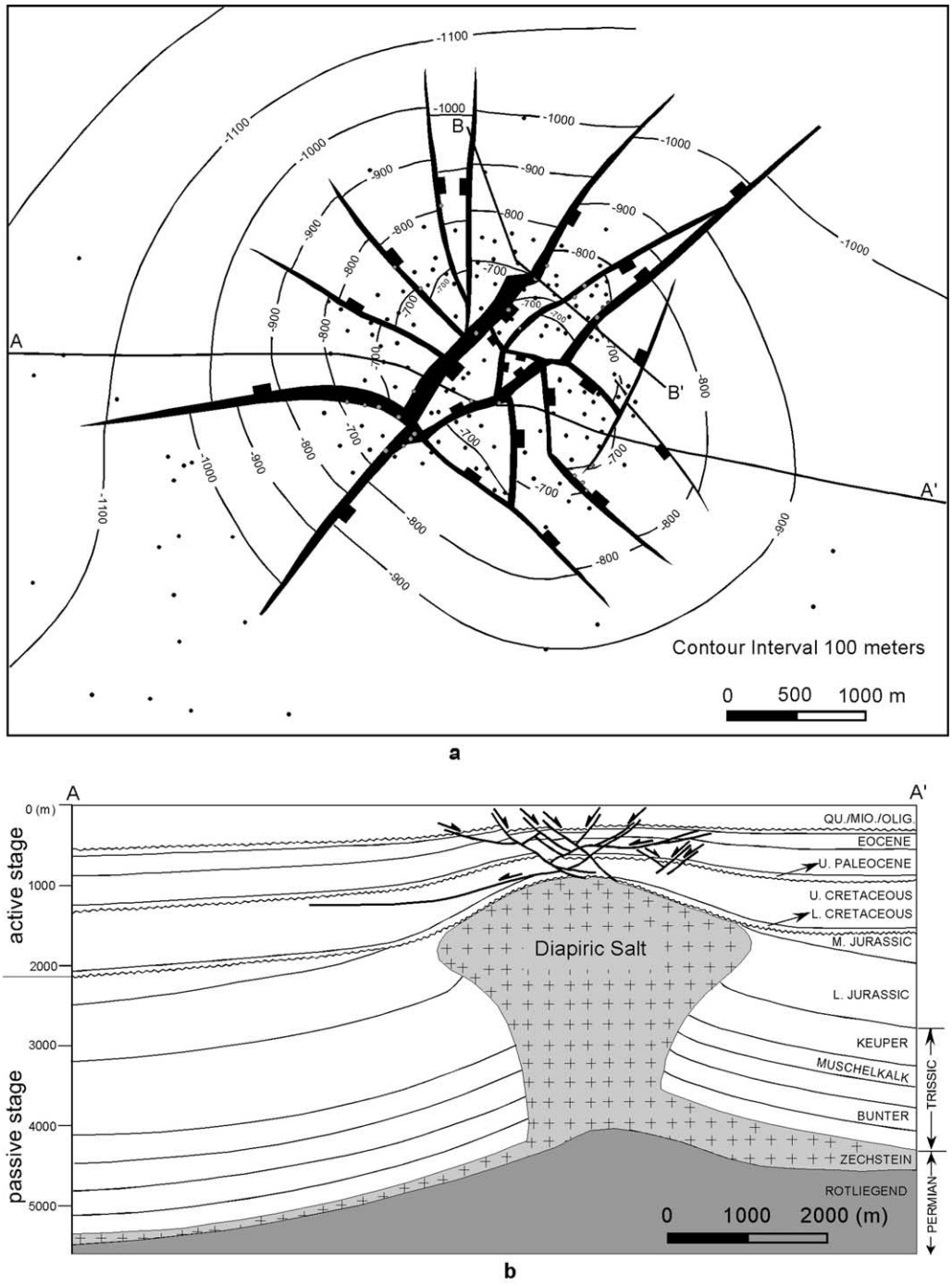

Fig. 2. Reitbrook dome, Northern Germany (after Schmitz and Flixeder, 1993). (a) Structure contour map drawn on the base of Tertiary (filled circles: well locations at mapped level). (b) Structure section A–A′.

salt domes, the Clay Creek dome in Texas, USA and the Reitbrook dome in Germany.

2. Structure of salt domes

Salt domes may be active, passive, reactive (Vendeville and Jackson, 1992) or dormant (Looff and Looff, 1999). Reactive, active, passive, and dormant diapirism are not mutually exclusive. They may exist at different stages of evolution within a single piercement structure based on the relative rate of upward salt movement, subsidence of the surrounding strata, and deposition of new sediments. The top of a passive diapir remains at the depositional interface and so does not have enough cover to form a dome (Barton, 1933; Seni and Jackson, 1983a,b). A reactive diapir forms in reaction to regional extension, causing the sedimentary cover of the diapir to be stretched and to

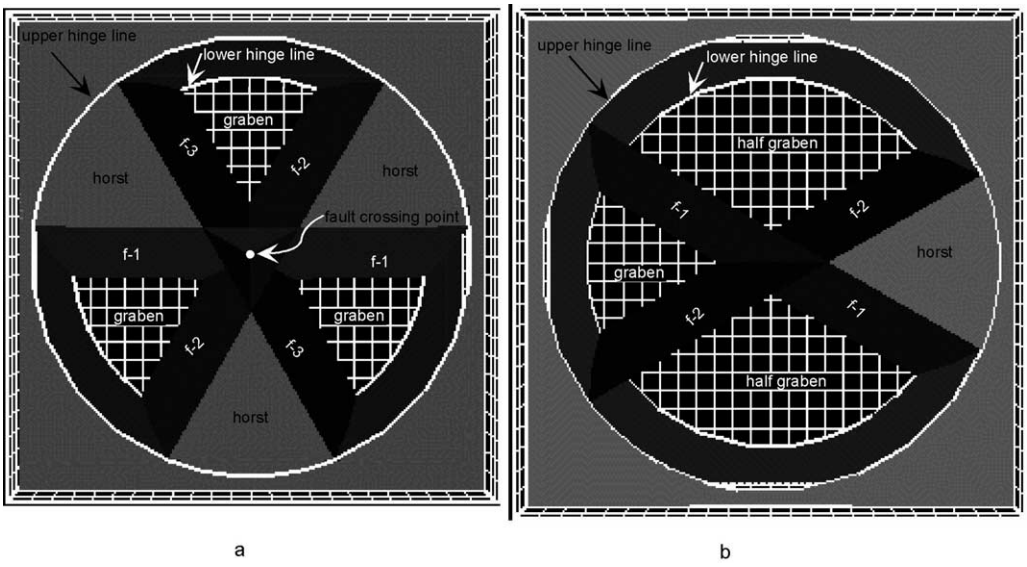

Fig. 3. Initial fault geometry in the model. (a) Y-pattern dome. (b) X-pattern dome.

subside below the regional level (Vendeville and Jackson, 1992). An active diapir forms a dome in which sedimentary units are uplifted above their regional elevation (Schultz-Ela et al., 1993). The active diapir stage is probably the most dynamic and complex in the salt dome growth history. An active diapir arches and uplifts the overburden strata above their regional elevation, where they may be removed by erosion. The structures of active diapirism have a better chance of preservation if the diapir only partly penetrates its overburden strata. The Clay Creek Dome (Fig. 1) in Washington County, TX (Ferguson and Minton, 1936; McDowell, 1951; Parker and McDowell, 1951, 1955) and the Reitbrook Dome (Fig. 2) in the North German salt basin (Schmitz and Flixeder, 1993) are typical examples of partly penetrating diapirs. Both domes provide well-documented examples of the 3D fault pattern in the strata arched over a salt dome. Both domes formed as a result of late diapir rise on a pre-existing piercement structure.

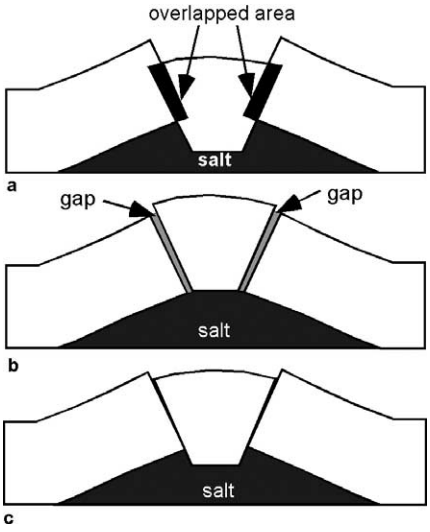

Fig. 4. Cross-section from model dome with faulted top of salt after 30° of horst block rotation. (a) Not enough uplift of the graben; the black regions adjacent to the faults indicate the overlapped area. (b) Too much uplift of the graben causes a gap. (c) Best fit between horst and graben blocks. The dip of the graben is 21.5°.

A review of published salt dome examples (Yin, 2003) indicates that the following features are characteristic of many active piercement structures. (1) The domes are circular or elliptical in map view. (2) Deformation of the domal roof initiates with either two or three master faults in the overburden strata. These faults are normal and radial, and intersect at or near the center of the dome. (3) The faults may sole into the top of a smooth salt intrusion or they may extend into the upper part of the salt intrusion. (4) A central graben may develop at the crest of the dome if three major normal faults are present. (5) The central graben is highly deformed by small faults, but remains constant in volume. (6) Individual flank horst and graben blocks are relatively unstrained and maintain constant area, thickness, and volume.

3. Kinematic model

The kinematic model for active domes discussed above is designed to maintain a constant volume. The primary deformation in the strata above salt is slip along faults, which is achieved by block rotation and radial flexural-slip (Yin, 2003).

Two or three crossing normal faults appear to be the minimum number of faults that will allow a circular dome to develop primarily by block rotations; thus our models begin

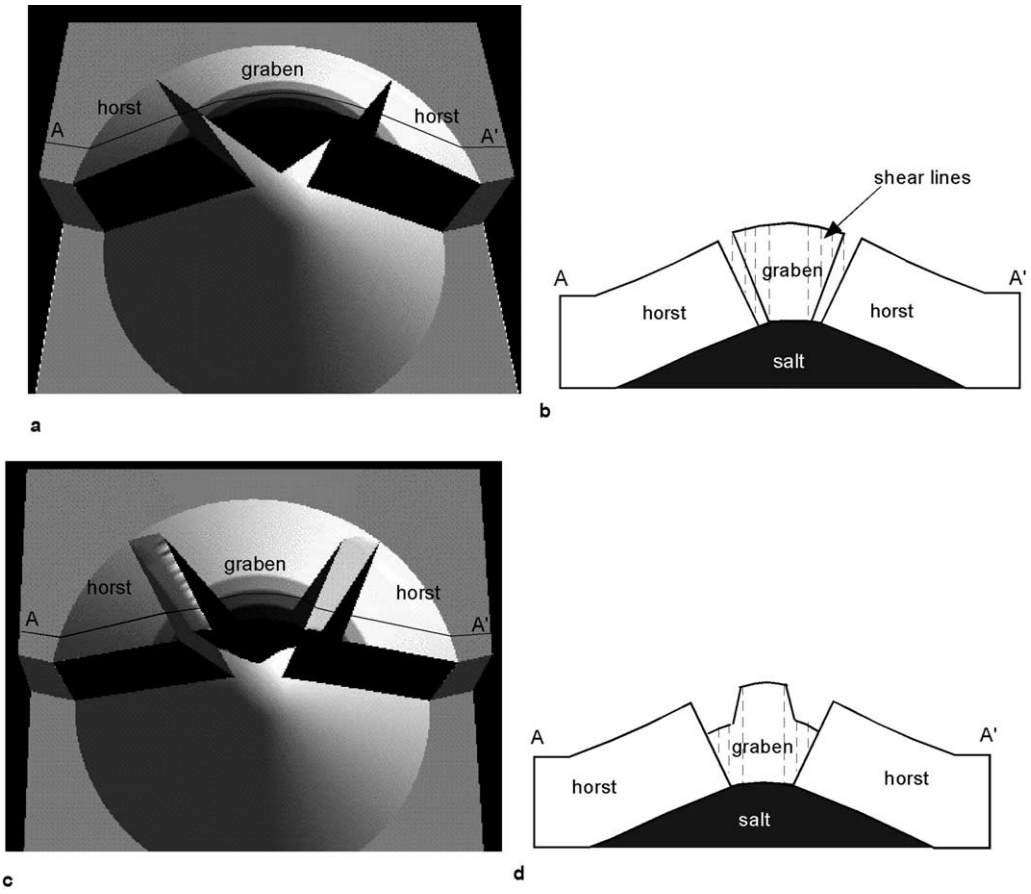

Fig. 5. Model with unfaulted top of salt. The horst and graben blocks dip radially 30° away from the crest of the dome. (a) Initial configuration of the model. (b) Cross-section from (a). (c) Model after closing the gap by vertical simple shear. (d) Cross-section from (c).

with these as the starting configuration. A Y-pattern dome initiates with three major normal faults (Fig. 3a). They are radially symmetrical and cut the dome into three horst blocks, three graben blocks, and a triangular central graben. The major faults cross each other, which results in a crossing point at or above the center of the dome. An X-pattern dome initiates with two major normal faults that cross at the crest of the dome (Fig. 3b). The faults cut the dome into one horst block, two half-graben blocks, and one graben block. No central graben develops in this configuration. If the top of the intruded salt is offset by faults, the horst and graben blocks undergo differential rotation. For any dip angle of the horst blocks, the models calculate the dip of the graben blocks by minimizing the gap and overlap space, where the grabens and horsts are in contact across a fault (Fig. 4). If the top of the intruded salt is smooth, the dip of the graben blocks equals the dip of the horst blocks. This configuration could result in wide gaps between horst and graben blocks. To simulate doming without piercement, vertical simple shear is used to close the gap between the blocks (Fig. 5). Other forms of deformation, e.g. oblique simple shear, could be used to close the gap and would produce a similar result.

4. Balancing and restoration of kinematic models

Both X- and Y-pattern models (Fig. 6) are restored in two and three dimensions. First we show the restoration of 2D sections from numerous orientations, and then show the restoration of models in 2.5D by map-surface unfolding.

4.1. Cross-section restoration: problems

The dome flanks are restored by line-length-constant flexural-slip, preserving thickness normal to the top surface of each unit (Brewer and Groshong, 1993). The central graben is restored by area balance. Restoration of the model results in apparently unbalanced cross-sections. Most sections across the flank grabens show apparent thickening because the section line is oblique to the dip (e.g. Fig. 7a–c). The central graben always shows unrestorable structural thinning because of out-of-plane volume transport (Fig. 7d). A radial cross-section that bisects a flank horst or graben is in the slip direction and thus has constant bed thickness and bed length except in the central graben (Fig. 7d). The apparent thickening of the flank blocks is small when the direction of the cross-section is close to the dip direction

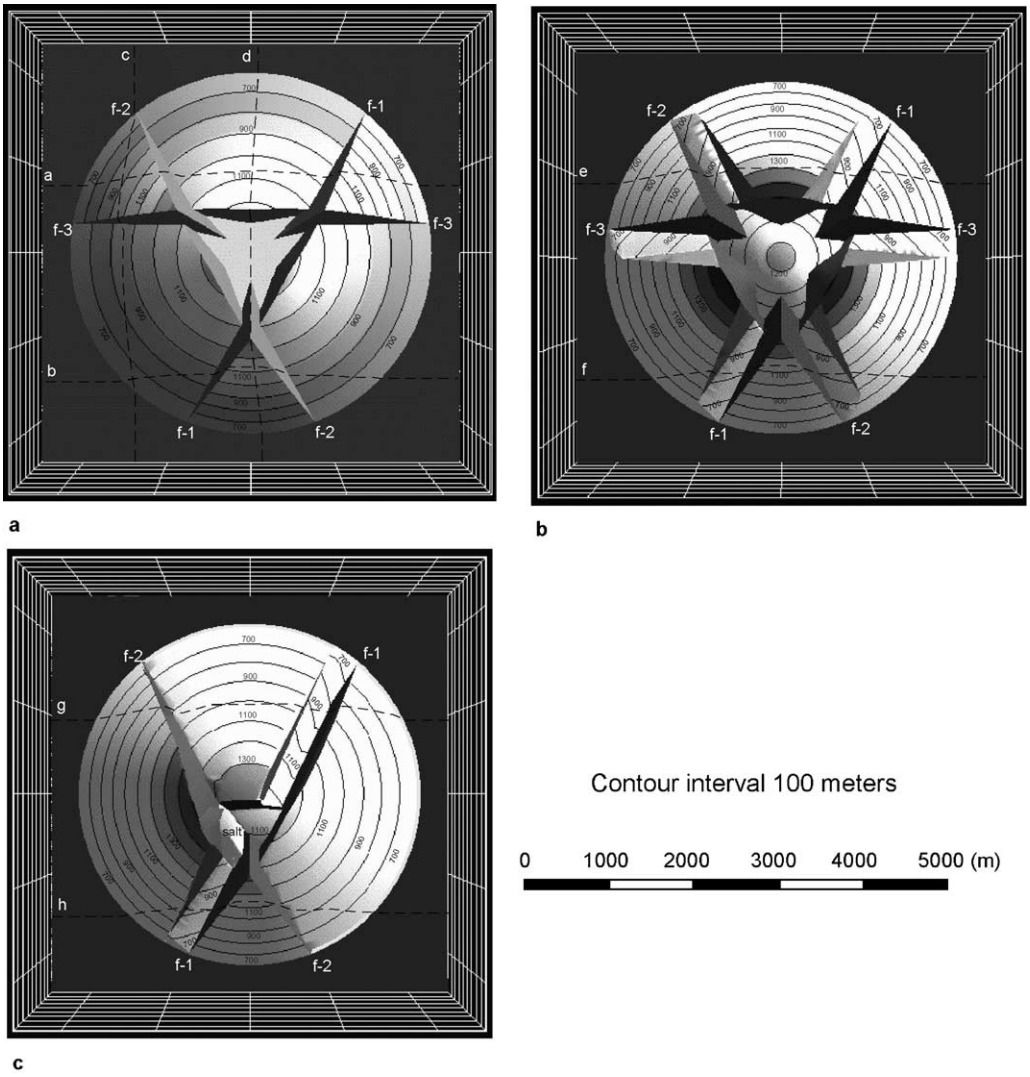

Fig. 6. Models to be restored. (a) Y-pattern model dome with faulted top of salt. (b) Y-pattern model dome with unfaulted top of salt. (c) X-pattern model dome with one fault (f-1) terminating against top of salt and the other one (f-2) offsetting top of salt.

(side blocks in Fig. 7a and b), but when the cross-section intersects the dip direction at a high angle (middle block in Fig. 7a and b), the thickening is very obvious.

4.2. Cross-section restoration: solutions

The apparent thickening can be removed by correcting the thickness of the cross-section according to the true dip in each block. The true thickness is calculated from

$$t = t_v \cos(\delta), \tag{1}$$

where t is the true thickness, and t_v is the vertical thickness of the section at the calculated location, and δ is the true dip of the block observed from the map (Groshong, 1999). Figs. 8–10 show the thickness-corrected restoration of cross-sections a–c from the Y-pattern model dome with faulted top of salt. With the thickness adjustment, the flexural-slip restoration results in cross-sections with constant bed thickness (Figs. 8b, 9b and 10b). After thickness adjustment, the restored sections a and c are correctly balanced (Figs. 8b and 10b). However, the restored section b shows obvious apparent regional extension (Fig. 9). This apparent regional extension is caused by the effect of out-of-plane material transport on the length of the section. To fix the apparent regional extension problem, the section can be restored with the pin lines placed in the undeformed material outside the dome (Fig. 9c and d). Fig. 9d shows restoration after correcting the thickness problem and fixing the apparent regional extension. Gaps along the faults result from an unrestorable out-of-plane transport.

Two cross-sections from the Y-pattern model with unfaulted top of salt are restored (Figs. 11 and 12). The horst blocks and the major part of the graben blocks are restored by flexural-slip as described previously. The minor parts of the graben sections, where the changes of thickness are most obvious, are restored by area balancing. The top of

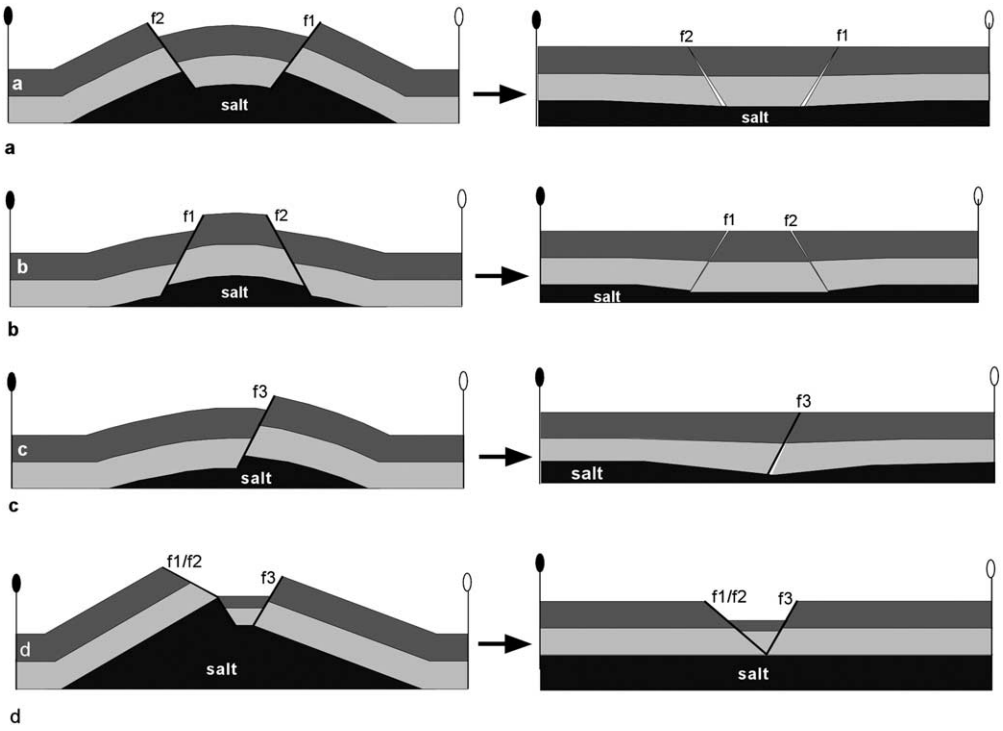

Fig. 7. Deformed-state and uncorrected restorations of cross-sections cut from a Y-pattern model dome with faulted top of salt (see Fig. 6a for location). In this and all subsequent cross-sections, pin lines have solid heads, loose lines have open heads. (a) Cross-section cut parallel to one major normal fault and perpendicular to the center line of one flank graben block. (b) Cross-section cut parallel to one major normal fault and perpendicular to the center line of one flank horst block. (c) Cross-section cut perpendicular to one major normal fault. (d) Cross-section cut through the central graben along the radial direction.

the adjacent horst blocks and the boundary fault planes are used as top and bottom of the minor block restoration. Without thickness adjustment, restoration of both sections results in cross-sections with obvious thickening suggesting growth sediments, especially in the middle block, where the section line intersects the dip direction at a high angle (Figs. 11b and 12b). The uncorrected section of Fig. 12b even implies growth reverse faults. After thickness correction, the restored cross-sections are balanced (Figs. 11c and 12c).

In the X-pattern model of Fig. 6c, fault f-2 offsets the top of salt and fault f-1 ends against the top of salt. The horst block and major part of the graben and half-graben blocks are restored by flexural-slip, while the minor part of the graben (Fig. 13a) and half-graben block (Fig. 14a) are restored by area balancing. Before thickness adjustment, both sections imply growth sedimentation (Figs. 13b and 14b), and Fig. 14b indicates reverse faulting. Using the corrected thickness, both cross-sections restore correctly (Figs. 13c and 14c).

4.3. Map-view restoration

In order to compare map-view restoration techniques, a Y-pattern model with faulted top of salt has been restored using vertical simple shear and parallel flexural-slip unfolding (Fig. 15). A perfect restoration would return the model to its original configuration (Fig. 15b). In the vertical simple-shear restoration, points on the bed surface are displaced vertically back to the regional elevation. The volume of the restored structure is preserved, but the area in map view is not preserved. The large gaps left in the restored model (Fig. 15c) indicate that vertical simple shear is not a good restoration method for 3D piercement structures deformed mainly by flexural-slip.

Parallel flexural-slip unfolding flattens the arched region and puts it back to the regional elevation. As a practical matter, map surface unfolding can only be accomplished as a computer application. We use the 3DMove software of the Midland Valley Company to perform the map surface

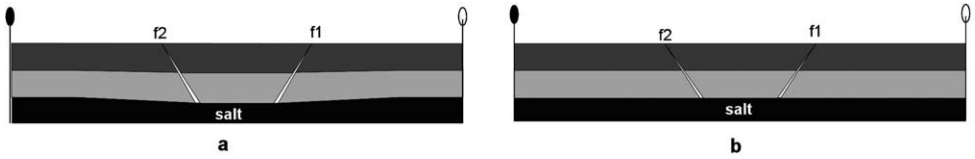

Fig. 8. Thickness-corrected restoration of cross-section a from the model dome with symmetrical Y-pattern faulting and faulted top of salt (see Fig. 7a for the original section). (a) Restored section before thickness adjustment. (b) Restored section after thickness adjustment.

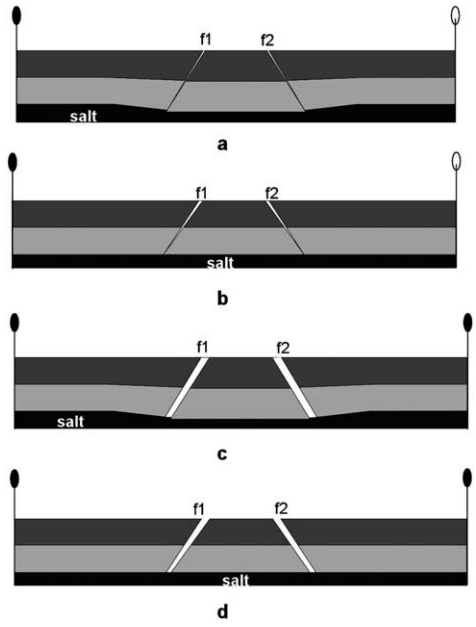

Fig. 9. Thickness-corrected restorations of cross-section b from the model dome with symmetrical Y-pattern faulting and faulted top of salt (see Fig. 7b for the original section). (a) Restored section before thickness adjustment. (b) Restored section after thickness adjustment. (c) Section restored with two pin lines before thickness adjustment. (d) Section restored with two pin lines after thickness adjustment.

restoration. In 3DMove, the region is unfolded along a unique direction for each fault block, whether or not the dip direction changes within the region. Each block is unfolded along its center line, the radial line that bisects the fault block, with the outer dome hinge line as a pin surface line (Fig. 15d). This algorithm maintains constant volume, constant bed thickness and constant length along the unfolding direction, and constant area in map view, but because it allows only one unique unfolding direction, it does not preserve length along the radial direction. Small gaps in the restored model (Fig.15d) indicate that parallel flexural-slip unfolding is a reasonably good method for 3D piercement structure restoration, although not a perfect one.

5. Balancing and restoration of the field examples

In order to test the applicability of the model results, two typical field examples of salt domes are restored in map and section.

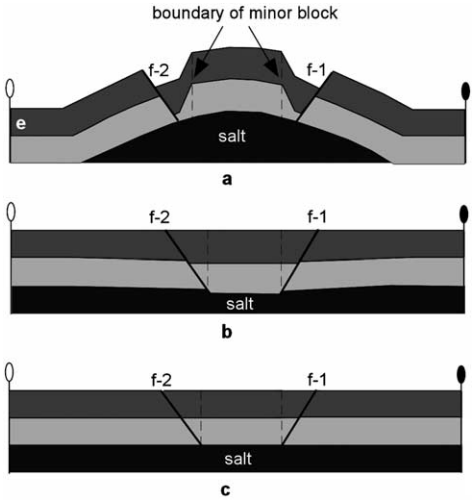

Fig. 11. Restoration of cross-section e of the model dome with symmetrical Y-pattern faulting and smooth top of salt (see Fig. 6b for location). (a) Original section. (b) Restored section before thickness adjustment. (c) Restored section after thickness adjustment.

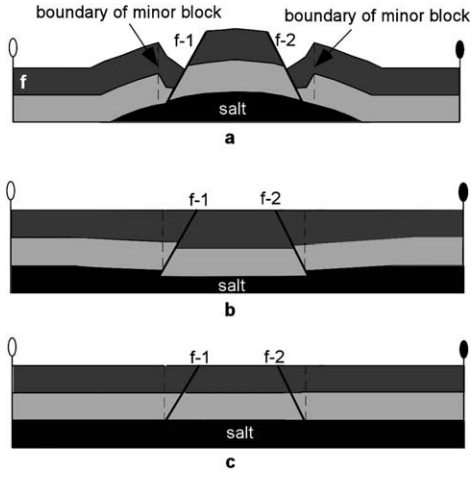

Fig. 12. Restoration of cross-section f of the model dome with symmetrical Y-pattern faulting and smooth top of salt (see Fig. 6b for location). (a) Original section. (b) Restored section before thickness adjustment. (c) Restored section after thickness adjustment.

5.1. Reitbrook dome

The Reitbrook dome is an asymmetrical Y-pattern salt dome with three major normal faults and numerous minor normal faults (Yin, 2003). The cross-section (Fig. 16a) from the Reitbrook dome (Fig. 2) created by Schmitz and

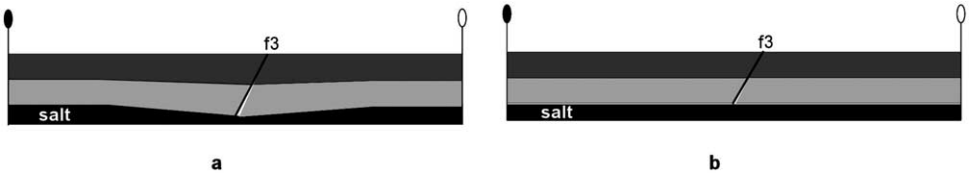

Fig. 10. Thickness-corrected restoration of cross-section c from the model dome with symmetrical Y-pattern faulting and faulted top of salt (see Fig. 7c for the original section). (a) Restored section before thickness adjustment. (b) Restored section after thickness adjustment.

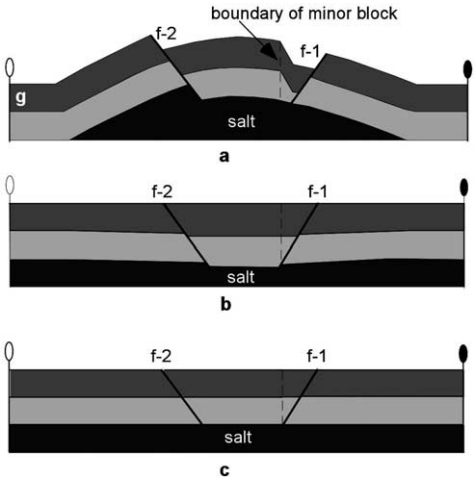

Fig. 13. Restoration of cross-section g of the model dome with X-pattern faulting (see Fig. 6c for location). (a) Original section. (b) Restored section before thickness adjustment. (c) Restored section after thickness adjustment.

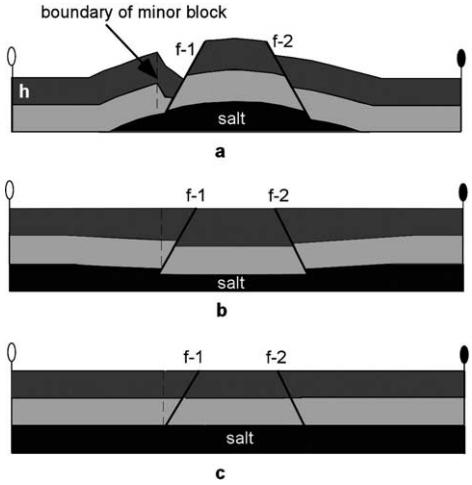

Fig. 14. Restoration of cross-section h of the model dome with X-pattern faulting (see Fig. 6c for location). (a) Original section. (b) Restored section before thickness adjustment. (c) Restored section after thickness adjustment.

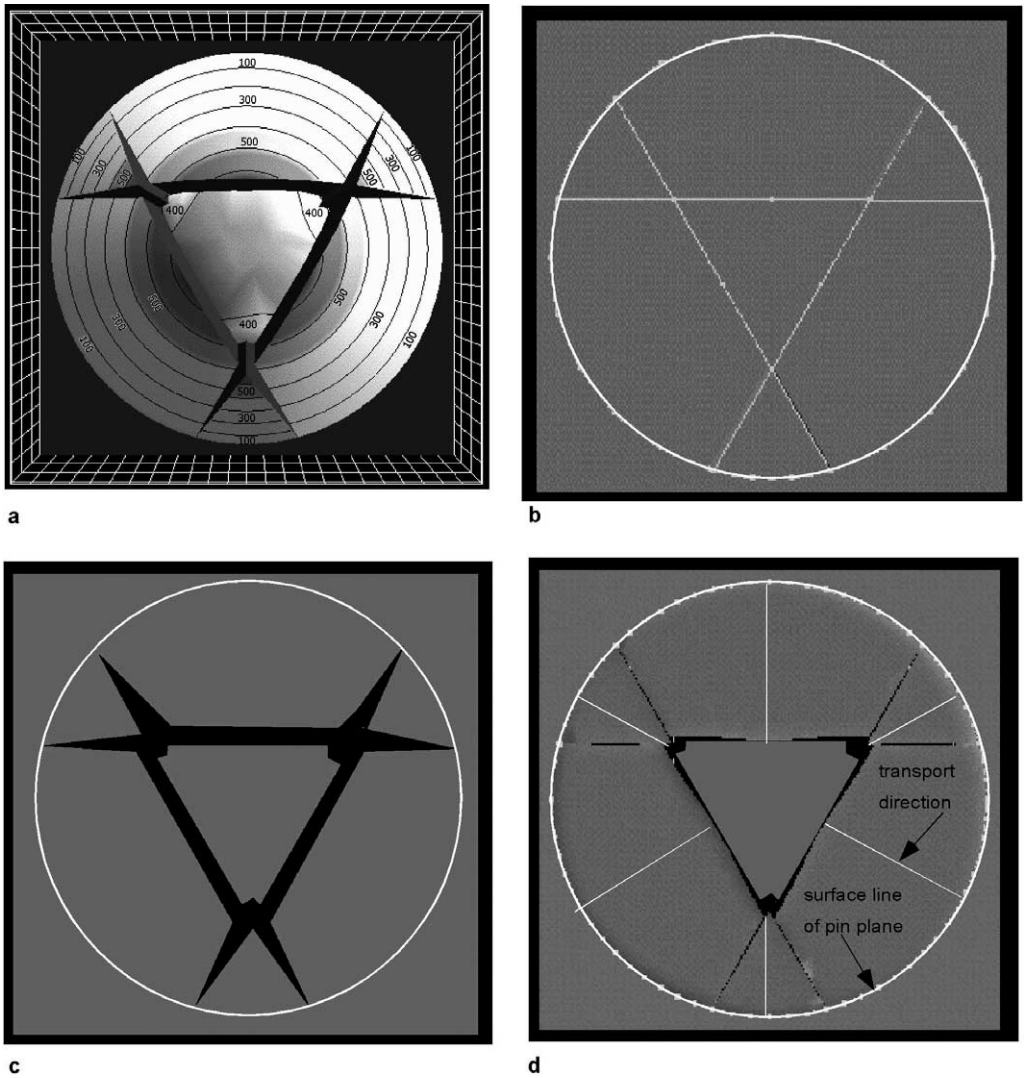

Fig. 15. Map-view restoration of top layer of a Y-pattern model dome with faulted top of salt. (a) 3D map view of the model. (b) Initial geometry before deformation. (c) Vertical simple shear restoration. (d) Parallel flexural-slip unfolding restoration.

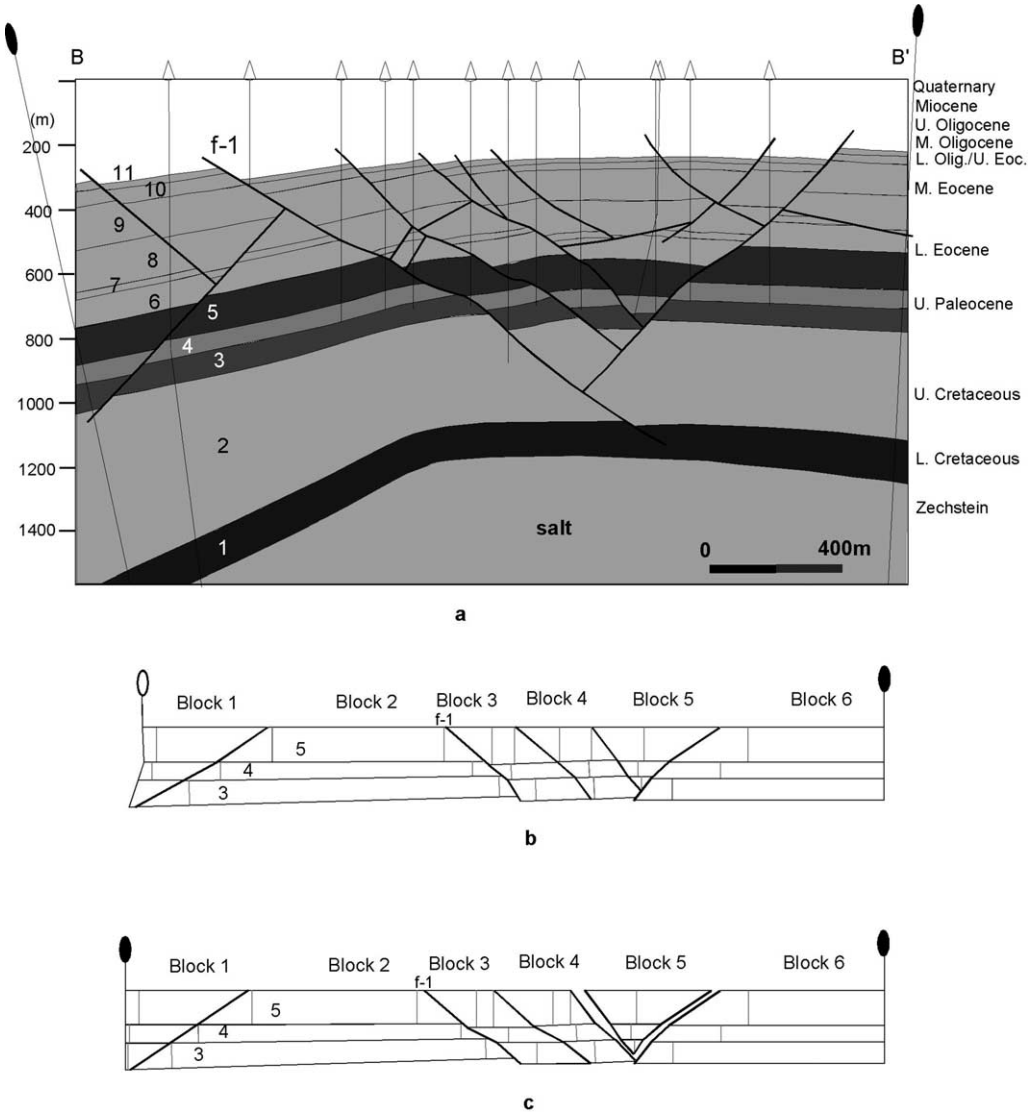

Fig. 16. Cross-section restoration of the Reitbrook salt dome. (a) Original cross-section (after Schmitz and Flixeder, 1993). For the location of the section, see Fig. 2a. (b) Original restored cross-section. (c) Restored section after correction for dip.

Flixeder (1993) is based on the correlation and projection of data from 13 wells. Units 3–5 have the most nearly constant thickness, implying that they most likely represent pre-growth units. To check the validity of the section and the applicability of the model result, these three units are restored.

First the thickness is corrected for dip with Eq. (1) using the block dips determined from Fig. 2a. The section was then restored by flexural-slip unfolding with a pin line on the right and a lose line on the left, resulting in a curved loose line (Fig. 16b). In the model, a cross-section is best restored by flexural-slip unfolding with a pin line at each end. When this technique is applied to the cross-section (Fig. 16c), gaps are observed, similar to those produced by the restoration of the model domes (Figs. 8 and 9). The gaps are caused by the effect of out-of-plane material transport and cannot be restored. Fault f-1 shows growth after thickness correction, and so is actually a growth fault, not an artifact. The restoration indicates that the section is well balanced.

The base of Tertiary in the Reitbrook dome is restored in map view using the parallel flexural-slip unfolding restoration algorithm of 3DMove. Major and minor normal faults divide the surface into more than 20 blocks. Each block has been unfolded and restored to the regional elevation along a transport direction parallel to its center line (Fig. 17a). For a block that covers the dome flank and extends to the outside edge of the model, the pin plane is set along its outside edge. For minor blocks that primarily cover the dome crest, the pin plane is set along one of its boundary faults. After unfolding, the flattened major blocks are fixed at their location, but the flattened minor blocks are translated and rotated until the best fit is obtained. The restored map of the Reitbrook dome (Fig. 17b) shows gaps along the fault traces. These gaps

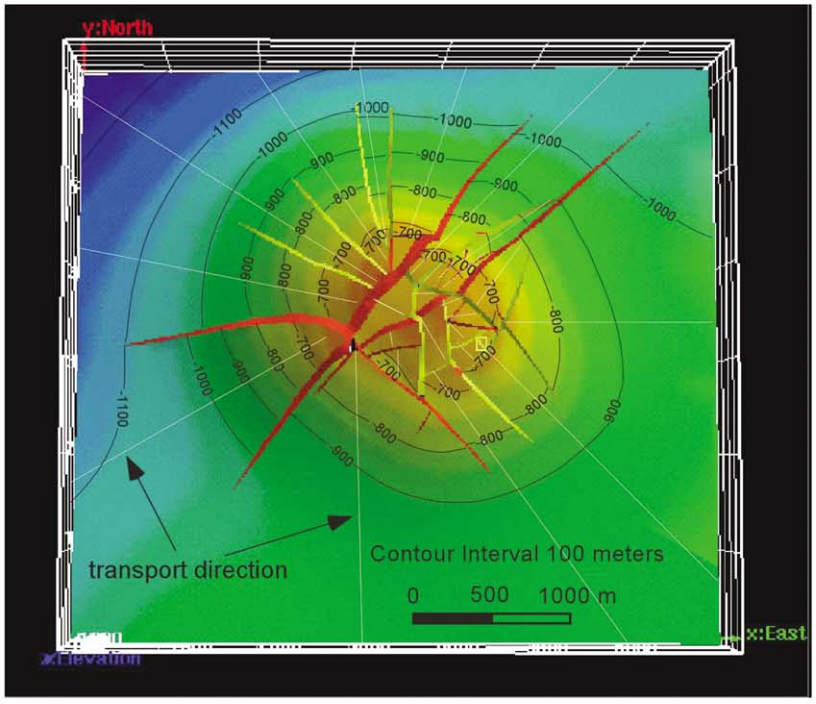

Fig. 17. Map view of the Reitbrook dome before and after restoration. (a) 3D structural reconstruction of the Reitbrook dome (data from Schmitz and Flixeder, 1993), showing transport directions used in unfolding. (b) Map-view restoration.

are mostly due to the use of the same unfolding direction for every block, similar to the gaps in the model dome restoration (Fig. 15d). The size of most gaps is comparable with the gap size observed in the model dome restoration (Fig. 15d). However, around the central graben above dome crest, the gaps are relatively big, indicating that the highly deformed central graben may include some undetected and therefore unrestored strains.

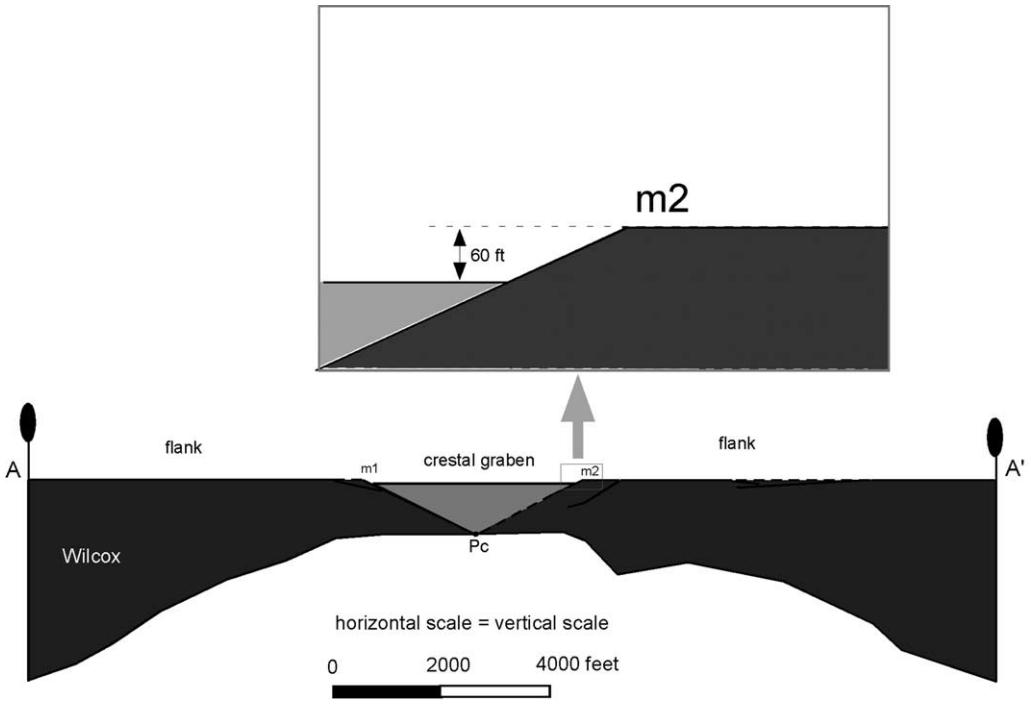

Fig. 18. Cross-section restoration of the Clay Creek dome (see Fig. 1 for location and original cross-section).

5.2. Clay Creek dome

The Clay Creek dome is a symmetrical Y-pattern salt dome with three major normal faults that cut the overburden strata into three grabens, three horsts, and a central graben. Each graben block is further deformed by minor normal faults as expected for faults detached on top of the salt (Yin, 2003).

Cross-section A–A′ is cut through the central graben, and nearly along the radial direction of the dome (Fig. 1a). Insights from model dome restoration show that the cross-section along the radial direction does not have an apparent thickening problem (Fig. 7d). Consequently, when we restore a radial-direction cross-section like cross-section A–A′ of Clay Creek dome (Fig. 1b), we do not need to correct the thickness. The flanks of the structure are relatively unstrained and restored by flexural-slip, and the crest is highly deformed and restored by area balancing. In the restoration to the top of Wilcox formation, the tips of flank blocks (points P1 and P2 in Fig. 1b) merge near the center of the crest (point Pc in Fig. 18), which implies that the crestal graben was originally triangle-shaped (Fig. 18). The top of the area-restored crestal graben is about 60 ft (20 m) lower than the top of the flank blocks. This unrestored thinning in the crest is presumably due to out of plain material transport as observed in the model dome cross-section restoration (Fig. 7d). The Wilcox formation on the flank is much thicker near the boundary of the cross-section than near the crest. Results from model domes show that the flanks of a radial cross-section should not have observable thickness change (Fig. 7d). The significant thickness change of the Wilcox formation on the dome flank is mostly due to the stratigraphic thinning over the crest, i.e. the Wilcox formation was deposited during dome uplift.

Top of the Wilcox Formation in the Clay creek dome is restored in map view using the same approach that we used in the Reitbrook dome restoration. The restored map of the Clay Creek dome (Fig. 19b) shows gaps along the fault traces. These gaps are referred to result from the use of the same unfolding direction for every block, as observed in the model dome restoration (Fig. 15d). The north and west part of the structure, where faults are distributed in a radial pattern, restores well (Fig. 19b). The size of the gaps is comparable with the gap size observed in the model dome restoration (Fig. 15d). The SE part of the dome, which has a more complicated fault pattern, does not restore as well as the NW part. The size of some gaps is relatively big and overlaps exist in the region near the central graben (Fig. 19b). Four of the five overlaps are located on the hanging wall of the tangential fault, indicating that a slight misinterpretation of the tangential fault may be the cause of the problem. Based on the geometric properties observed from Y-pattern model domes, we suggest an alternative interpretation (Yin and Groshong, 2003). In the revised interpretation, the tangential fault is reinterpreted to terminate against the major normal fault (Fig. 20) instead of separating one major normal fault into two disconnected parts (Fig. 19). The restoration of the revised map (Fig. 20b) has smaller gaps and much smaller overlap regions.

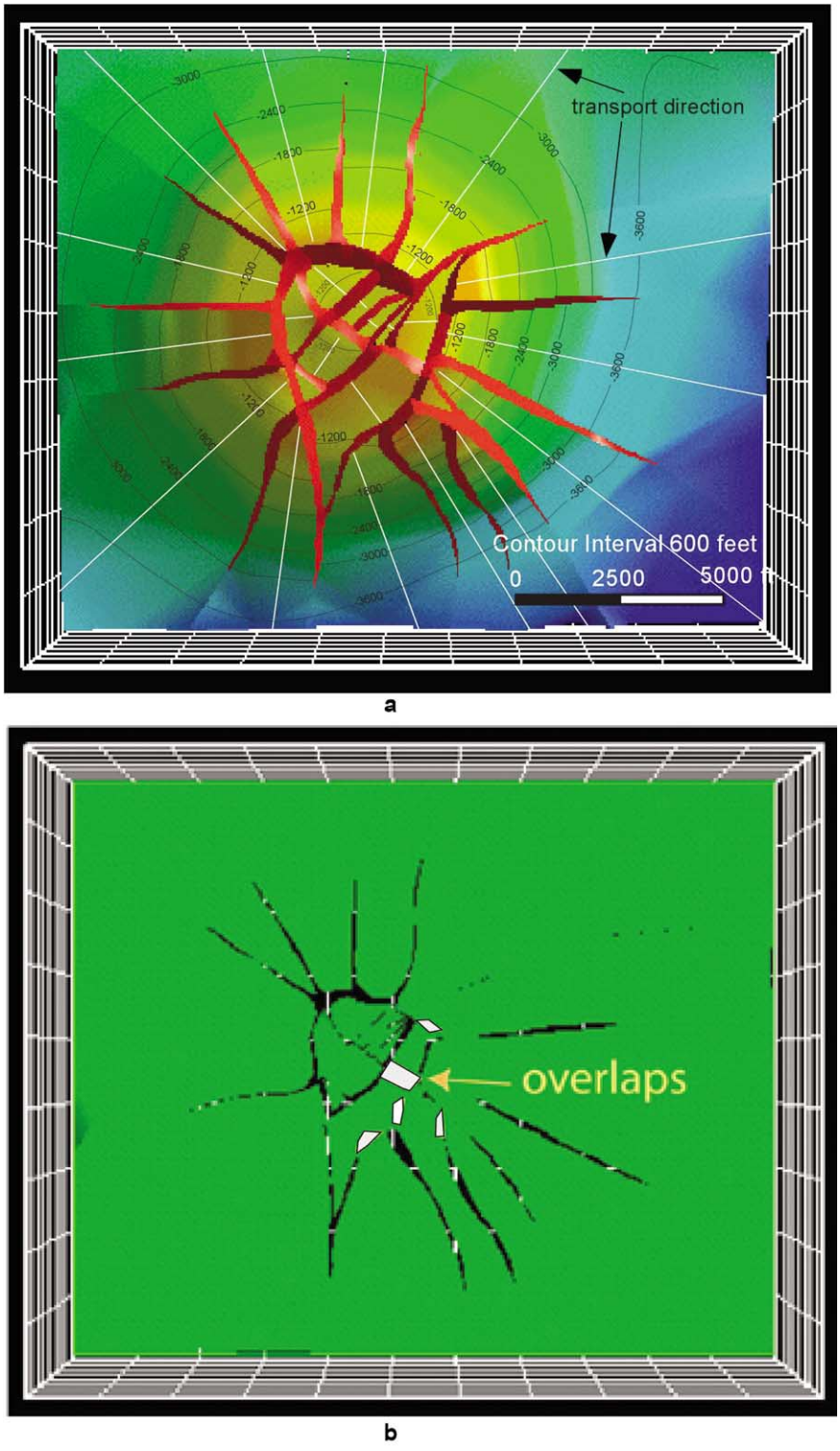

Fig. 19. Map view of the Clay Creek dome before and after restoration. (a) 3D structural reconstruction of the Clay Creek dome (data from McDowell, 1951), showing transport directions used in unfolding. (b) Map-view restoration.

6. Summary and conclusions

In this paper, we have restored sections and surfaces of balanced 3D flexural-slip models that we derived based on the properties of active piercement structures. 2D section restoration of the model shows that cross-sections of highly 3D structures are almost always apparently unbalanced. The restored model sections include obvious gaps along faults.

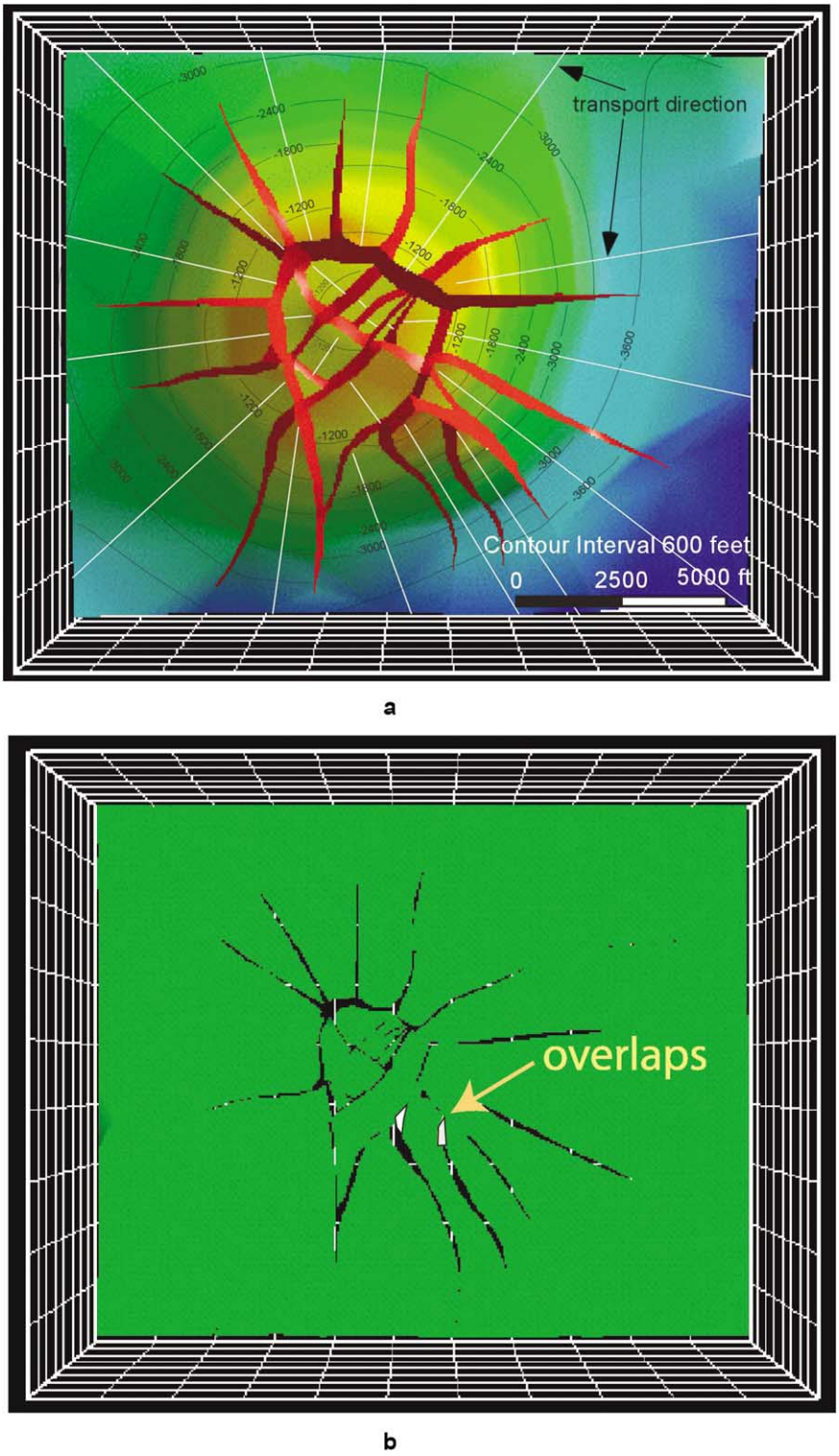

Fig. 20. Map view of the reinterpreted Clay Creek dome before and after restoration. (a) 3D structural reconstruction of the Clay Creek dome (reinterpreted from McDowell, 1951). (b) Map-view restoration.

When it occurs in 2D structures, large fault gap in the restored section is a clear indication that the section is unbalanced and not valid. However, fault gaps in restored sections of highly 3D structures result from the unrestorable out-of-plane volume transport, and hence not necessary the indication that the section are not valid. 2D restoration shows that most sections of the model include apparent thickening, which could be easily misinterpreted as representing stratigraphic growth during deformation. This paper indicates that the apparent thickening can be fixed by

correcting thicknesses using the dip magnitude as determined from the map view. Apparent regional extension is another possible problem that may occur when 2D section restoration technique is applied to highly 3D structures. To fix the apparent regional extension problem, the section can be restored with pin lines placed in the undeformed material outside the dome.

The model surfaces are restored in map view using vertical simple shear and parallel flexural-slip unfolding. Vertical simple shear restoration resulted in a restored surface with large fault-trace gaps, while small gaps exist in the restored surface using parallel flexural-slip unfolding. This paper shows that parallel flexural-slip unfolding is a better and acceptable technique when applied to map-view restoration of highly 3D structures.

We have applied the insight from model results to validate the interpretation of the Clay Creek dome and the Reitbrook dome. The restoration shows that the interpretation of these two domes is mostly reasonable and valid, although a small modification is suggested for the Clay Creek dome.

Acknowledgements

The authors wish to thank the Midland Valley Company for the use of software 3DMove, and John Spang at Texas A&M University for providing a copy of McDowell's thesis on the Clay Creek dome, and J. Schmitz for providing salt dome data in Reitbrook, Germany. This research has been supported in part by DOE grant DE-FC02-91ER75678, Contract DE-FC26-00NT40927, National Natural Science Foundation of China Contract No. 40402019 and by a Graduate Council Fellowship from the University of Alabama to the senior author. R.H. Groshong is grateful for support from Jiafu Qi, Director, Key Laboratory for Hydrocarbon Accumulation Mechanism, China Petroleum University, People's Republic of China, National Natural Science Foundation of China Contract No. 40372072 and Ministry of Education Contract No. 200303. Comments by reviewers Martin Jackson and Scott Youngs greatly assisted in improving the clarity of the text. We have benefited from discussions of 3D models with Oscar Fernandez.

References

Barr, D., 1985. 3-D palinspastic restoration of normal faults in the Inner Moray Firth: implications for extensional basin development. Earth and Planetary Science Letters 75, 191–203.

Barton, D.C., 1933. Mechanics of formation of salt domes with special reference to Gulf coast salt domes of Texas and Louisiana. American Association of Petroleum Geologists Bulletin 17, 1025–1083.

Brewer, R.C., Groshong Jr., R.H., 1993. Restoration of cross-sections above intrusive salt domes. American Association of Petroleum Geologists Bulletin 77, 1769–1780.

Buddin, T.S., Kane, S.J., Williams, G.D., Egan, S.S., 1997. A sensitivity analysis of 3-dimensional restoration techniques using vertical and inclined shear constructions. Tectonophysics 269, 33–50.

Chamberlin, R.T., 1910. The Appalachian folds of central Pennsylvania. Journal of Geology 18, 228–251.

Dahlstrom, C.D.A., 1969. Balanced cross-sections. Canadian Journal of Earth Sciences 6, 743–757.

Ferguson, W.B., Minton, J.W., 1936. Clay Creek salt dome, Washington County, Texas. American Association of Petroleum Geologists Bulletin 20, 68–90.

Gibbs, A.D., 1983. Balanced section constructions from seismic sections in areas of extensional tectonics. Journal of Structural Geology 5, 153–160.

Gratier, J.-P., Gullier, B., 1993. Compatibility constraints on folded and faulted strata and calculation of total displacement using computational restoration (UNFOLD program). Journal of Structural Geology 15, 391–402.

Gratier, J.-P., Gullier, B., Delorme, A., Odonne, F., 1991. Restoration and balance of a folded and faulted surface by best-fitting of finite elements: principle and applications. Journal of Structural Geology 13, 111–115.

Groshong Jr., R.H., 1999. 3-D Structural Geology. Springer, Heidelberg.

Hossack, J.R., 1995. Geometric rules of section balancing for salt structures. In: Jackson, M.P.A., Roberts, D.G., Snelson, S. (Eds.), Salt Tectonics: A Global Perspective. American Association of Petroleum Geologists Memoir 65, pp. 29–40.

Kerr, H., White, N., 1996. Application of an inverse method for calculating three dimensional fault geometries and slip vectors, Num River field, Nigeria. American Association of Petroleum Geologist Bulletin 80, 432–444.

Kerr, H., White, N., Brun, J.P., 1993. An automatic method for determining three-dimensional normal fault geometry. Journal of Geophysical Research 98, 17837–17858.

Looff, K.M., Looff, K.M., 1999. Possible geologic influence on salt falls associated with the storage caverns at Bryan Mound, Brazoria County, Texas. Gulf Coast Association of Geological Societies Transactions 49, 322–331.

McDowell, A.N., 1951. The origin of the structural depression above Gulf Coast salt domes with particular reference to Clay Creek dome, Washington County, Texas. MS Thesis, Texas A&M University.

Parker, T.J., McDowell, A.N., 1951. Scale model as guide to interpretation of salt dome faulting. American Association of Petroleum Geologists Bulletin 35, 2076–2086.

Parker, T.J., McDowell, A.N., 1955. Model studies of salt-dome tectonics. American Association of Petroleum Geologists Bulletin 39, 2384–2470.

Rouby, D., Cobbold, P.R., Szatmari, P., Demerican, S., Coelho, D., Rici, J.A., 1993. Least-squares palinspastic restoration of regions of normal faulting—application to the Campos basin (Brasil). Tectonophysics 221, 439–452.

Rouby, D., Xiao, H., Suppe, J., 2000. 3-D restoration of complexly folded and faulted surfaces using multiple unfolding mechanisms. American Association of Petroleum Geologists Bulletin 84, 805–829.

Rowan, M.G., Kligfield, R., 1989. Cross-section restoration and balancing as an aid to seismic interpretation in extensional terranes. American Association of Petroleum Geologists Bulletin 73, 955–966.

Schmitz, J., Flixeder, F., 1993. Structure of a classic chalk oil field and production enhancement by horizontal drilling, Reitbrook, NW Germany. In: Spencer, A.M. (Ed.), Generation. Accumulation and Production of Europe's Hydrocarbons III. Special Publication of the European Association of Petroleum Geoscientists, vol. 3, pp. 144–154.

Schultz-Ela, D.D., Jackson, M.P.A., Vendeville, B.C., 1993. Mechanics of active salt diapirism. Tectonophysics 228, 275–312.

Seni, S.J., Jackson, M.P.A., 1983a. Evolution of salt structures, East Texas diapir province, part 1, sedimentary record of halokinesis. American Association of Petroleum Geologists Bulletin 67, 1219–1244.

Seni, S.J., Jackson, M.P.A., 1983b. Evolution of salt structures, East Texas diapir province, part 2, patterns and rates of halokinesis. American Association of Petroleum Geologists Bulletin 67, 1245–1274.

Vendeville, B.C., Jackson, M.P.A., 1992. The rise of diapirs during thin-skinned extension. Marine and Petroleum Geology 9, 331–353.

White, N., Jackson, J.A., McKenzie, D.P., 1986. The relationship between the geometry of normal faults and that of the sedimentary layers in their hanging walls. Journal of Structural Geology 8, 897–909.

Williams, G.D., Kane, S.J., Buddin, T.S., Richards, A.J., 1997. Restoration and balance of complex folded and faulted rock volumes: flexural flattening, jigsaw fitting and decompaction in three dimensions. Tectonophysics 273, 203–218.

Woodward, N.B., Boyer, S.E., Suppe, J., 1989. Balanced geological cross-sections: an essential technique in geological research and exploration. American Geophysical Union, Short Course in Geology 6.

Yin, H., 2003. Structural interpretation and validation of three-dimensional piercement structures. PhD Dissertation, University of Alabama, Tuscaloosa, Alabama.

Yin, H., Groshong, R.H., 2003. Geometric properties of active piercement structures: geologic insight from 3-D kinematic models. Gulf Coast Association of Geological Society Transactions 53, 887–899.